The authors are indebted to the National Science Council of the Republic of China for financial support through grant NSC76-0208-M007-30. JMS acknowledges also the Conselho Nacional de Pesquisas e Desenvolvimento of Brazil for providing a graduate fellowship.

References

BETHE, H. (1928). *Ann. Phys. (Leipzig)*, **87**, 55-129.
CHANG, S. L. (1981). *Appl. Phys.* A**26**, 221-226.
CHANG, S. L. (1982*a*). *Phys. Rev. Lett.* **48**, 163-166.
CHANG, S. L. (1982*b*). *Acta Cryst.* A**38**, 516-521.
CHANG, S. L. (1984). *Multiple Diffraction of X-rays in Crystals.* Berlin, Heidelberg, New York, Tokyo: Springer-Verlag.
CHANG, S. L. (1986). *Phys. Rev. B*, **33**, 5848-5850.
CHANG, S. L. (1987). *Crystallogr. Rev.* **1**, 87-189.
CHANG, S. L. & VALLADARES, J. A. P. (1985). *Appl. Phys.* A**37**, 57-64.
CHAPMAN, L. D., YODER, D. R. & COLELLA, R. (1981). *Phys. Rev. Lett.* **46**, 1578-1581.
COLE, H., CHAMBERS, F. W. & DUUN, H. M. (1962). *Acta Cryst.* **15**, 138-144.
COLELLA, R. (1974). *Acta Cryst.* A**30**, 413-423.
GONG, P. P. & POST, B. (1983). *Acta Cryst.* A**39**, 719-724.
HART, M. & LANG, A. R. (1961). *Phys. Rev. Lett.* **7**, 120-121.
HØIER, R. & AANESTAD, A. (1981). *Acta Cryst.* A**37**, 787-794.
HØIER, R. & MARTHINSEN, K. (1983). *Acta Cryst.* A**39**, 854-860.
HÜMMER, K. & BILLY, H. W. (1982). *Acta Cryst.* A**38**, 841-848.
HÜMMER, K. & BILLY, H. W. (1986). *Acta Cryst.* A**42**, 127-133.
JAGODZINSKI, H. (1980). *Acta Cryst.* A**36**, 104-116.
JURETSCHKE, H. J. (1982*a*). *Phys. Rev. Lett.* **48**, 1487-1489.
JURETSCHKE, H. J. (1982*b*). *Phys. Lett. A*, **92**, 183-185.
KAMBE, K. & MIYAKE, S. (1954). *Acta Cryst.* **7**, 218-219.
LAUE, M. VON (1931). *Ergeb. Exakten Naturwiss.* **10**, 133-158.
MIYAKE, S. & OHTSUKI, Y. H. (1974). *Acta Cryst.* A**30**, 103-104.
POST, B. (1977). *Phys. Rev. Lett.* **39**, 760-763.
POST, B. (1983). *Acta Cryst.* A**39**, 711-718.
POST, B., GONG, P. P., KERN, L. & LADELL, J. (1986). *Acta Cryst.* A**42**, 178-184.
RENNINGER, M. (1937). *Z. Phys.* **106**, 141-176.
SCHMIDT, M. C. & COLELLA, R. (1985). *Phys. Rev. Lett.* **55**, 715-717.
SHEN, Q. (1986). *Acta Cryst.* A**42**, 525-533.

Acta Cryst. (1988). A**44**, 70-75

Electron Diffraction Patterns of Chrysotile: Effect of Specimen Orientation

BY J. E. CHISHOLM

Department of Mineralogy, British Museum (Natural History), Cromwell Road, London SW7 5BD, England

(*Received* 16 *May* 1987; *accepted* 17 *September* 1987)

Abstract

Electron diffraction patterns of chrysotile asbestos fibrils should have the $2mm$ symmetry of a rotation photograph because the layers in the structure are curled as cylinders. The way in which the fibril orientation affects the diffraction patterns is considered theoretically. The departures from ideal symmetry attributable to specimen orientation are noted: they affect mainly the $h00$ reflections close to the fibre axis. Actual diffraction patterns show a consistent difference in the separation of the $h0l$-$h0\bar{l}$ pairs on the upper levels, and $\bar{h}0l$-$\bar{h}0\bar{l}$ pairs on the lower. The experimental conclusion [Yada (1979). *Can. Mineral.* **17**, 679-691] that this difference is not an effect of specimen orientation is confirmed theoretically but its cause remains obscure.

Introduction

The serpentine minerals are hydrated magnesium silicates, $Mg_3Si_2O_5(OH)_4$, with structures which consist of composite layers parallel to (001). In these, a layer of SiO_4 tetrahedra shares the apical oxygen atoms with a layer of $Mg(OH,O)_6$ octahedra. However, the octahedral magnesium hydroxide layer has a and b dimensions which are a little larger than those of the silicate layer. The resulting strain is relieved by curling of the composite layers with the (larger) magnesium hydroxide layer on the outside. In the variety of serpentine known as chrysotile, the composite layers curl about the a axis and wrap around this axis to form the tiny cylinders which are the asbestos fibrils.

The theory of diffraction from cylindrical lattices (and arrangements related to them, such as spirals and helices) was developed by Jagodzinski & Kunze (1954) and in a series of papers by Whittaker (1954, 1955*a*, *b*, 1956, 1957, 1963), who also determined the detailed atomic arrangement in chrysotile. X-ray fibre diffraction photographs, and later electron diffraction patterns, showed the features expected for cylindrical wrapping of the composite layers. Whittaker's deductions were strikingly confirmed by the high-resolution electron micrographs of Yada (1967, 1971) which showed directly the wrapping of the layers about the axis of the cylindrical fibrils.

The wrapping of layers around the axis of a cylinder implies that diffraction patterns from a stationary fibre should have the $2mm$ symmetry of a rotation photograph. X-ray fibre patterns do indeed have this

0108-7673/88/010070-06$03.00

symmetry but electron diffraction patterns do not: Yada (1979) has described the departures from the expected $2mm$ symmetry in detail. Many workers must have observed these departures from rotational symmetry and probably dismissed them as effects of specimen orientation. But Yada examined the effect of tilting the fibril experimentally and showed that orientation only accounted for some of the asymmetry. This paper gives the corresponding theoretical treatment of specimen orientation and its effect on the geometry of the chrysotile electron diffraction pattern. The classical principles of diffraction crystallography, the reciprocal lattice and the Ewald construction, are applied to an unusual problem.

The Fourier transform of a cylindrical lattice

The two common polytypes of chrysotile, $2M_{c1}$ and $2Or_{c1}$, both have two-layer stacking sequences (Wicks & Whittaker, 1975) and are usually called clinochrysotile and orthochrysotile. Most of the discussion which follows is concerned with clinochrysotile, the most common polytype. Analogous behaviour is expected for orthochrysotile: the main differences will be noted at each stage in the discussion.

In deriving the expected electron diffraction patterns, the following cylindrical lattice dimensions are used: a 5·34, c 14·64 Å; β 93·3° for clinochrysotile (β 90° for orthochrysotile). The cylindrical lattice is formed by curling a two-dimensional generating lattice (a-b); that generating lattice is centred and this has the same effect on the diffraction behaviour as C-face centring in an ordinary lattice.

Whittaker's discussion of chrysotile diffraction patterns considered a monoclinic cylindrical lattice, which is now usually defined with a as the cylinder axis, b around the circumference and c^* as the radial direction. The Fourier transform of such a lattice (Fig. 1) has two main components: (i) sharp maxima at circles centred on the a axis, corresponding to $h0l$ reflections; and (ii) an intensity distribution associated with circles centred on the a axis corresponding to $hk0$ reflections. The form of the intensity distribution depends on the average radius and the internal diameter of the cylinder, and on the way the layers are wrapped (circularly, spirally or helically, for example).

Diffraction patterns of chrysotile consist of prominent 5·34 Å a-axis layer lines. The centring means that sharp $h0l$ spots are observed only on the h even levels; the 'flared' $hk0$ reflections occur alone on the h odd levels. The combination of the monoclinic symmetry of clinochrysotile and the $2mm$ rotational symmetry gives $h00$ reflections and pairs of reflections $h0l$–$h0\bar{l}$ on either side of the a axis (Fig. 2a). For clinochrysotile, the $h0l$ reflections with l odd are weak and seldom observed because successive layers in the two-layer stacking sequence differ only very slightly

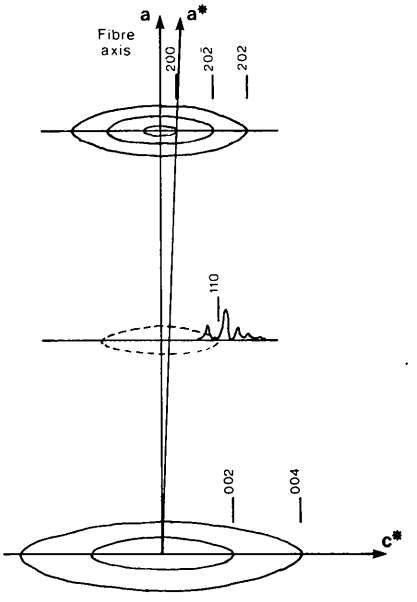

Fig. 1. The Fourier transform of a monoclinic cylindrical lattice consists of (i) sharp $h0l$ maxima at circles centred on the a axis, and (ii) an intensity distribution associated with $hk0$ circles centred on the a axis. The lattice is centred; the $h0l$ maxima with l odd (such as 201, 20$\bar{1}$) are not shown as they are only occasionally visible on diffraction patterns.

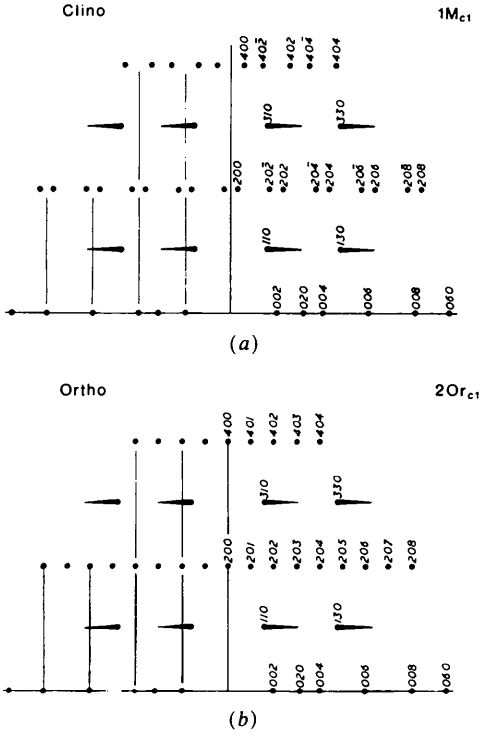

Fig. 2. Simplified theoretical diffraction patterns of (a) clinochrysotile, (b) orthochrysotile, with sharp $h0l$ spots and flared $hk0$ maxima. Only the upper half of each diffraction pattern is shown: the lower should be related by the expected $2mm$ symmetry. [Based on Figs. 2(d) and (e) of Zussman, Brindley & Comer (1957).]

in their displacement (Wicks & Whittaker, 1975). Reflections with l odd are therefore not shown on Fig. 2(a) and are not considered further for clinochrysotile.

The orthochrysotile Fourier transform is similar to that of clinochrysotile but the $h0l$ and $h0\bar{l}$ circles coincide because of the orthorhombic character. The $h00$ reflections lie on the a axis and there are now single $h0l$ reflections forming a rectangular mesh (Fig 2b). Successive layers in the stacking sequence are rotated by 180° and reflections with l odd are sufficiently intense to be observed except on the zero level.

Our main concern here will be the sharp $h0l$ maxima, (i), since (a) their positions can be measured accurately on diffraction patterns, and (b) the asymmetry of $h0l$-$h0\bar{l}$ pairs of spots can be recognized by eye. The sharp $h0l$ maxima occur at circles defined by the cylindrical polar coordinates, ξ and ζ:

$$\xi = lc^* + ha^* \cos \beta^* \qquad (1)$$

$$\zeta = ha^* \sin \beta^*. \qquad (2)$$

The intensity distribution, (ii), associated with $hk0$ leads to fine structure in the 'flared' $hk0$ reflections, the observation of which confirmed the essential correctness of the cylindrical lattice model. The position of the $hk0$ 'flared' maxima is affected by fibril orientation in the same way as the $h0l$ reflections. However, the diffuseness and variable fine structure of the $hk0$ reflections tend to conceal the small shift in position and make it difficult to measure. The $hk0$ reflections are therefore not considered in any detail here.

Ewald plane approximation

Because of the very short wavelength of the electrons, it is usual to approximate the reflecting sphere, whose radius can be taken as proportional to $1/\lambda$, by a plane, perpendicular to the electron beam, which we shall call the Ewald plane. When the fibre axis of chrysotile is perpendicular to the electron beam, the film coordinates x, y are simply the cylindrical polar coordinates ξ, ζ scaled by λD (D = effective camera length of the electron microscope).

Let us suppose that the chrysotile fibre axis a is tilted by an angle μ away from the position perpendicular to the electron beam. The new reciprocal-lattice coordinate ζ' perpendicular to the electron beam and in the plane containing it and the fibre axis is

$$\zeta' = \zeta/\cos \mu = ha^* \sin \beta^*/\cos \mu. \qquad (3)$$

Instead of cutting the $h0l$ circles in a diameter, the Ewald plane now cuts them in a chord at a distance $\zeta \tan \mu$ ($= ha^* \sin \beta^* \tan \mu = \zeta' \sin \mu$) from the centre. The new reciprocal-lattice coordinate ξ' at right angles to the electron beam and the fibre axis is then given by Pythagoras' theorem:

$$\xi'^2 = \xi^2 - \zeta^2 \tan^2 \mu$$

with ξ and ζ given by (1) and (2).

With the aid of a small computer and a graph plotter, it is easy to draw the diffraction pattern expected for any fibre orientation specified by μ. The diffraction pattern coordinates x, y are simply ξ', ζ' scaled by λD. The angles on the diffraction pattern corresponding to $2(\beta - 90)$ in the reciprocal lattice are calculated from the coordinates x, y. The calculated angles for $h0l$-$h0\bar{l}$ pairs are those subtended at $00l$: for $\mu < 5°$, the difference between this angle and that subtended at the point where the perpendicular bisector of the pair cuts the zero level is negligible, being much less than the error of measurement.

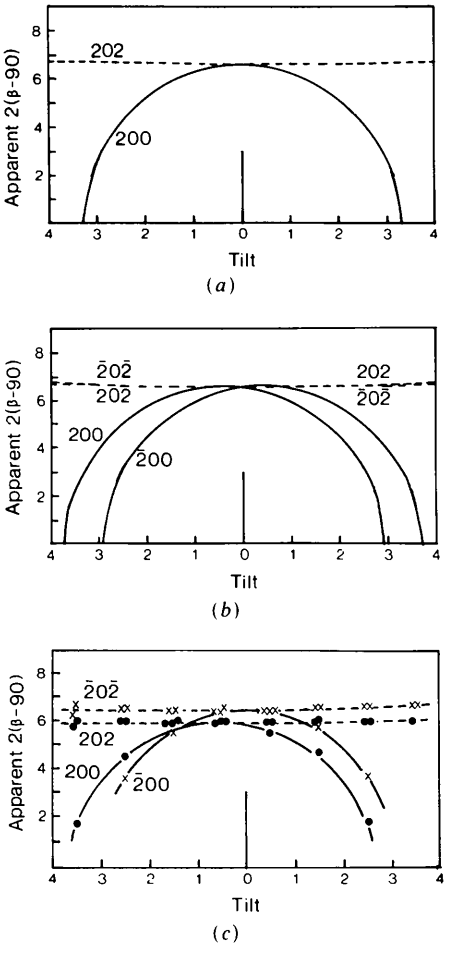

Fig. 3. Variation with specimen tilt (in degrees) of the apparent $2(\beta - 90)$ angle (in degrees) subtended at the origin by the 200 pairs and at 002 by the 202-$20\bar{2}$ pairs on clinochrysotile diffraction patterns: (a) as predicted using the Ewald plane approximation; (b) as predicted using the Ewald sphere for 100 kV electrons (λ = 0·037 Å); (c) as found experimentally [redrawn from Yada (1979) with the zero-tilt position midway between the maxima of his curves for 200 and $\bar{2}00$].

The effect of tilt on the apparent $2(\beta-90)$ angle is shown in Fig. 3(a). As the specimen is tilted, all reflections move closer to the vertical axis because $\xi' < \xi$ and this occurs symmetrically on the upper and lower levels. The effect is most obvious for the $h00$ pairs which move closer together as the tilt increases, reducing the apparent $2(\beta-90)$ angle. The calculated $2(\beta-90)$ angle for the $h0l$-$h0\bar{l}$ pairs (*e.g.* 202-20$\bar{2}$) hardly changes as the specimen is tilted, although both reflections themselves move closer to the vertical axis of the pattern. When the tilt exceeds $(\beta-90)$, 3·3°, the $h00$ reflections are no longer observed since the Ewald plane has passed outside the $h00$ circles. Diffraction patterns with one or both $h00$ or $\bar{h}00$ reflections missing are sometimes observed.

For orthochrysotile, $\beta = 90°$ and very little tilt is needed for the $h00$ spots to disappear (how much tilt depends on the size and profile of the maximum in the Fourier transform). Some diffraction patterns of orthochrysotile do have one or both these $h00$ spots missing.

The curve (Fig. 3a) showing the variation of apparent $2(\beta-90)$ with tilt predicted by the Ewald plane approximation does not match Yada's (1979) experimental results (Fig. 3c). The differences in $2(\beta-90)$ between the upper and lower levels are not explained by the Ewald plane approximation, either for the $h00$ or the $h0l$-$h0\bar{l}$ pairs. However, the approximation does predict that the separation of the 200 spots is very sensitive to tilt whereas that of the 202-20$\bar{2}$ pairs is hardly affected. This is qualitatively similar to the effect of tilting observed by Yada (1979) but is symmetrical on the upper and lower levels.

Ewald sphere and specimen orientation

In considering the geometry of the Ewald sphere intersecting the Fourier transform of a cylindrical lattice, it is convenient to use the analogy with rotation photographs. Consider the electron microscope as a diffraction camera. The geometry of a chrysotile diffraction pattern is that of a flat-plate rotation photograph. The film coordinates x, y have been derived in terms of the reciprocal-lattice coordinates ξ, ζ by Buerger (1942, pp. 141–142).

The case where the fibre axis is not perpendicular to the electron beam is that of inclined-beam geometry and has much in common with the geometry of Weissenberg photographs in the general case (Buerger, 1942, pp. 296–299). An analogous problem is the geometry of the equi-inclination rotation X-ray photographs used by Whittaker (1953) to explore the central regions of the upper reciprocal-lattice levels, inaccessible by conventional photography.

If the fibre axis of chrysotile is tilted by an angle μ from the position perpendicular to the incident beam, the geometry is as shown in Fig. 4. The radius of the zero-level reflecting circle is

$$R_0 = \cos\mu$$

and the radius of the reflecting circle on the nth level is

$$R_n = \cos\nu.$$

From Fig. 4,

$$\sin\nu = \zeta + \sin\mu$$

and

$$\nu = \arcsin(\zeta + \sin\mu). \tag{4}$$

Remembering that the film is at right angles to the incident beam, even though the beam is inclined to the fibre axis, we can derive the y film coordinate since $\sin(\nu-\mu)$ is the analogue of ζ in the normal beam case and

$$y = D\sin(\nu-\mu)/\cos 2\theta$$

for flat-plate geometry. Substituting for $\cos 2\theta$ (Buerger, 1942, p. 139), we find

$$y = \frac{2D\sin(\nu-\mu)}{(2-\zeta^2-\xi^2)}. \tag{5}$$

The x film coordinate is derived from flat-plate geometry as

$$x = D\tan\Upsilon \tag{6}$$

(Buerger, 1942, p. 141) and for general inclined-beam geometry

$$\Upsilon = \arccos\left[\frac{\cos^2\mu + \cos^2\nu - \xi^2}{2\cos\mu\cos\nu}\right] \tag{7}$$

(Buerger, 1942, p. 299).

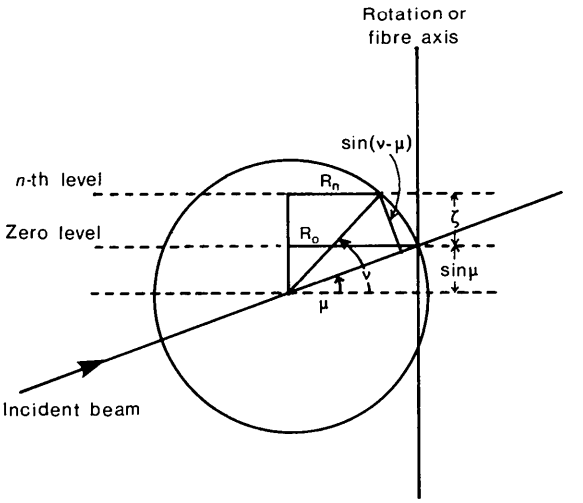

Fig. 4. General inclined-beam diffraction geometry normal to the plane containing the incident beam and the rotation axis (fibre axis) [based on Fig. 157, p. 297 of Buerger (1942)].

Equations (4)-(7) make it possible to calculate the film coordinates x, y for any angle of tilt μ from the values of ξ and ζ derived from the cell dimensions [equations (1) and (2)]. Angles on the diffraction pattern can then be calculated from the film coordinates. The angles corresponding to $2(\beta-90)$ in the reciprocal lattice are those subtended at the $00l$ spot on the diffraction pattern by the $h0l$-$h0\bar{l}$ pair in each case.

Diffraction patterns for 100 kV electrons have been calculated for a series of tilts μ and the effect of tilt on the apparent $2(\beta-90)$ angle for the 200 and 202-20$\bar{2}$ pairs is shown in Fig. 3(b). As before, the separation of $h00$ pairs of spots is reduced when the fibril is tilted but the reflecting sphere treatment shows that the 200 and $\bar{2}00$ pairs are differently affected. As the tilt angle is increased, first one pair {200} disappears and then the other.

Again the 202-20$\bar{2}$ pairs have an apparent $2(\beta-90)$ which scarcely alters as the fibril is tilted. Both reflections move closer to the vertical axis of the pattern, but by slightly different amounts on the upper and lower levels. The $2mm$ symmetry of a rotation photograph is thus lost on tilting: the horizontal mirror line disappears and with it the diad rotation point (Fig. 5a). The calculated patterns, however, do not account quantitatively for the differences between the upper and lower levels which are actually found. Most observed diffraction patterns are like Fig. 5(b) and have both the 200 and $\bar{2}00$ spots present. The tilt angle in these cases must therefore be less than 2·9° (Fig. 3b). Consider the apparent $2(\beta-90)$ angles of the 202-20$\bar{2}$ and $\bar{2}02$-$\bar{2}0\bar{2}$ pairs on the upper and lower levels of these patterns. The observed differences between these angles on the upper and lower levels are an order of magnitude larger (0·5° or more) than the predicted differences (0·04° or less). In addition, Yada's (1979) results (Fig. 3c) show that the observed differences between the upper and lower levels for these pairs are almost independent of tilt angle. Similarly, if one compares the theoretical and experimental tilting curves (Figs. 3b and c) for the {200} reflections, the apparent $2(\beta-90)$ angles for 200 and $\bar{2}00$ differ at zero tilt and the effect of tilting seems to be superimposed on this difference.

The theory described explains the behaviour observed by Yada (1979) when chrysotile fibrils are tilted. But the consistent differences he observed in the separation of all $h0l$-$h0\bar{l}$ pairs on the upper and lower levels cannot be accounted for by specimen orientation.

For orthochrysotile, the reflecting sphere and inclined-beam geometry predict the absence of $h00$ spots at zero tilt and each of those spots should appear at one precise orientation only, the equi-inclination angle for their layer line. Since the $h00$ maxima are not δ functions but have a definite extent in reciprocal space, the $h00$ spots will in fact be seen over a small

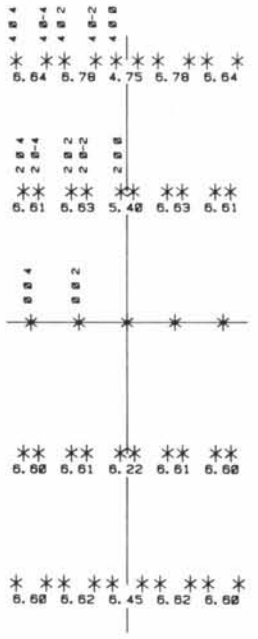

(a)

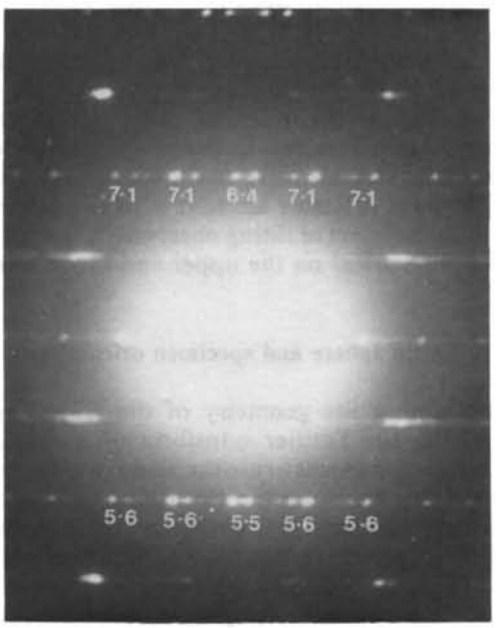

(b)

Fig. 5. (a) Sharp $h0l$ spots on a diffraction pattern calculated using the Ewald sphere (100 kV electrons, $\lambda = 0{\cdot}037$ Å) and inclined-beam geometry for a clinochrysotile fibril with the fibre axis tilted 1·5° out of the plane perpendicular to the incident electron beam. The calculated angle subtended at $00l$ by each $h0l$-$h0\bar{l}$ pair (at the origin by each $h00$ pair) is shown; this angle on the diffraction pattern corresponds to $2(\beta-90)$ in the reciprocal lattice. (b) Electron diffraction pattern of chrysotile from Jeffrey mine, Asbestos, Quebec, with the apparent $2(\beta-90)$ angles (subtended at $00l$ by the $h0l$-$h0\bar{l}$ pairs) measured. As both 200 and $\bar{2}00$ are present, the tilt of the fibril axis out of the plane perpendicular to the electron beam must be less than 2·9° (*cf.* Fig. 3b).

range of orientations. The $h0l$ spots will be displaced slightly towards the vertical axis of the pattern by an amount which decreases with distance from that axis.

Concluding remarks

The theory given here shows which departures from $2mm$ rotational symmetry on chrysotile electron diffraction patterns can be attributed to specimen orientation. Apart from the initial differences between the upper and lower levels, the theory successfully explains the behaviour of the electron diffraction patterns as the specimen is tilted about an axis perpendicular to the fibre axis and to the electron beam. The results of Yada's (1979) tilting experiments are thus confirmed by theory. Specifically, the theory accounts for the sensitivity of the $h00$ reflections to tilting of the chrysotile fibril. Differences in fibril orientation relative to the electron beam will cause the separation of the $h00$ pairs to differ on either side of the origin, as is often observed in addition to the systematic differences between the upper and lower levels. In more extreme cases, the $h00$ pair on one side of the origin, or those on both, may be absent and this too sometimes occurs on observed diffraction patterns.

But the consistent differences in the separation and the apparent $2(\beta-90)$ angle of the $h0l$-$h0\bar{l}$ pairs on the upper and lower levels (Fig. 5*b*) remain unexplained. The theory confirms the experimental conclusion of Yada (1979) that these differences do not result from or depend on the specimen orientation. Differences of the observed magnitude are not observed on electron diffraction patterns of other materials and therefore cannot be attributed to instrumental aberrations.

The theoretical treatment assumes kinematical diffraction based on the generally accepted idea of cylindrical wrapping of the layers in chrysotile. An explanation of the differences between the upper and lower levels is unlikely to be found in dynamical diffraction theory. Dynamical effects will alter the diffracted intensities but not the geometry of the spot positions and should in any case be small because the fibril diameter (200–300 Å) is almost certainly less than the extinction distance.

Yada & Iishi (1977) have invoked refraction to account for fine structure observed in the $00l$ reflections of chrysotile. But the differences between the upper and lower levels are unlikely to be explicable in terms of refraction. If that were the cause, those differences would be similar for all chrysotile fibrils. In fact, they vary markedly from one fibril to another. The fine structure noted by Yada & Iishi (1977) is not necessarily the result of refraction as it can equally well be accounted for by diffraction from a cylindrical arrangement of layers (Whittaker, 1954, 1963).

It is possible that the actual Fourier transform differs in some way from that of a monoclinic cylindrical lattice. If so, this would imply some kind of departure from simple cylindrical wrapping of the layers in chrysotile. The differences between the upper and lower levels are observed in both cylindrical and helically wrapped fibrils, the latter being recognizable by the splitting of the $hk0$ 'flared' reflections (Whittaker, 1955*b*; Whittaker & Zussman, 1971). Conical wrapping of the layers in chrysotile will not explain the observed differences either, as it leads simply to two sets of levels slightly inclined to each other because the two halves of the fibril have their fibre axes in different directions. Yada & Iishi (1977) show a diffraction pattern of this kind (their Fig. 13) from a chrysotile with 'cone-in-cone' appearance. The monoclinic cylindrical lattice model for chrysotile has been very fully tested (see the series of papers by Whittaker) and further confirmed by high-resolution transmission electron microscopy (Yada, 1967, 1971). The model is very successful in accounting for the distinctive features of chrysotile diffraction patterns. If there is some kind of departure from the monoclinic cylindrical lattice model, it must therefore be a comparatively subtle one, perhaps related to the exact wrapping of the layers or to bending or distortion of the chrysotile fibrils.

I should like to thank Dr E. J. W. Whittaker for his encouragement, careful comments and patient explanations which removed many errors and misconceptions. I am also grateful to my colleague David Kempe for his encouragement.

References

BUERGER, M. J. (1942). *X-ray Crystallography.* New York: John Wiley.
JAGODZINSKI, H. & KUNZE, G. (1954). *Neues Jahrb. Mineral. Monatsh.* pp. 95-108, 113-130, 137-150.
WHITTAKER, E. J. W. (1953). *Acta Cryst.* **6**, 93.
WHITTAKER, E. J. W. (1954). *Acta Cryst.* **7**, 827-832.
WHITTAKER, E. J. W. (1955*a*). *Acta Cryst.* **8**, 261-265, 265-271, 571-574.
WHITTAKER, E. J. W. (1955*b*). *Acta Cryst.* **8**, 726-729.
WHITTAKER, E. J. W. (1956). *Acta Cryst.* **9**, 855-862, 862-864.
WHITTAKER, E. J. W. (1957). *Acta Cryst.* **10**, 149-156.
WHITTAKER, E. J. W. (1963). *Acta Cryst.* **16**, 486-490.
WHITTAKER, E. J. W. & ZUSSMAN, J. (1971). *The Electron-optical Investigation of Clays*, edited by J. A. GARD, pp. 176-177. London: Mineralogical Society.
WICKS, F. J. & WHITTAKER, E. J. W. (1975). *Can. Mineral.* **13**, 227-243.
YADA, K. (1967). *Acta Cryst.* **23**, 704-707.
YADA, K. (1971). *Acta Cryst.* A**27**, 659-664.
YADA, K. (1979). *Can. Mineral.* **17**, 679-691.
YADA, K. & IISHI, K. (1977). *Am. Mineral.* **62**, 958-965.
ZUSSMAN, J., BRINDLEY, G. W. & COMER, J. J. (1957). *Am. Mineral.* **42**, 133-153.

Acta Cryst. (1988). A44, 76-78

A Lattice-Dynamical Comparison of Nonbonded Potential Parameters for Hydrocarbons

BY A. CRIADO AND R. MARQUEZ

Departamento de Optica e Instituto de Ciencia de los Materiales, Universidad de Sevilla, Aptdo 1065, 41080 *Seville, Spain*

(*Received* 16 *June* 1987; *accepted* 17 *September* 1987)

Abstract

The crystallographic thermal parameters have been calculated with a lattice-dynamical procedure for some hydrocarbons in the rigid-body appproximation using some sets of potential parameters taken from the literature. A comparison with experimental data confirms that the well known Williams IV*b* set is very good for describing vibrational properties in polycyclic hydrocarbons.

Introduction

The calculation of crystallographic thermal parameters using a lattice-dynamical approach with empirical potential energy functions has become a routine procedure nowadays. Although some work has been done with heteroatom compounds (Dianez, Criado, Lopez-Castro & Marquez, 1986) the most successful results have been obtained on hydrocarbons because a large number of potential sets have been derived [for a review see Mirsky (1978)] which correctly reproduce the static properties of these compounds. A possible explanation for this success may be that the intermolecular forces in hydrocarbons are well described by r^6 and exp potential models, other interactions, mainly Coulombic, being small in comparison. Evidently, this is not the case for nitrogen (Williams & Cox, 1984) or oxygen (Cox, Hsu & Williams, 1981) compounds where electrostatic interactions are important.

The most extensive contribution in this field has been made by Filippini, Gramaccioli, Simonetta & Suffritti, who made in 1973 a comparison of different potential sets and concluded that the so-called Williams IV*b* set (Williams, 1967)* gives the best agreement with experiment. Since then, this set has been adopted in most calculations, which currently include the contribution of internal modes described by appropriate intramolecular fields (Filippini & Gramaccioli, 1986).

The purpose of this paper is to make an updated comparison of the best potential sets which are available in the literature nowadays. For such a comparison, some particular hydrocarbons have been extensively studied, such as naphthalene and anthracene (Gramaccioli & Filippini, 1983) and for these the results are satisfactory. In order to extend the number of experimental results we consider some additional 'rigid-body' compounds taken from recent literature which gives accurate structure determinations.

Potential sets

Since the only potentials of importance are van der Waals interactions we have selected five different sets of so-called '6-exp' functions which are shown in Table 1. Sets (*a*), (*b*) and (*e*) were derived by Williams (1966, 1967; Williams & Starr, 1977) by fitting crystal structure parameters (non-vibrational). Set (*c*) was derived by Warshel & Karplus (1972) together with an intramolecular potential field to be applied in conformational analysis. Set (*d*) was derived by Mirskaya, Kozlova & Bereznitskaya (1974) (see also Mirsky, 1978). Because of the large number of compounds involved in the fits these sets [except (*d*)] are among the most reliable which can be found in the literature.

Method of calculation

The individual crystallographic thermal parameters (Willis & Pryor, 1975) were obtained from the **T**, **L** and **S** tensors (Schomaker & Trueblood, 1968) calculated by sampling the Brillouin zone and summing the contributions of the allowed vibrational modes. These were found by diagonalization of the dynamical matrix (Born & Huang, 1954) constructed in the quasi-harmonic and rigid-body approximations considering interactions up to a limit of 6 Å. The C–H bond distances were normalized to 1·08 Å, maintaining the experimental bond angles in order to get a better agreement with experiment. A previous energy-minization procedure was necessary in order to achieve the equilibrium configuration. The program *WMIN* (Busing, 1972) was used to perform the Newton-Raphson steps. A more detailed description of the method can be found elsewhere (Criado, Conde & Marquez, 1984).

* This set is indicated by Filippini *et al.* and other authors as IV*a* instead of IV*b*.

0108-7673/88/010076-03$03.00